Molecular dynamics simulations of ordered alkane chains physisorbed on graphite

Reinhard Hentschke, Britta L. Schürmann, and Jürgen P. Rabe
Max-Planck-Institut für Polymerforschung, Postfach 3148, W-6500 Mainz, Germany

(Received 26 November 1991; accepted 9 January 1992)

Scanning tunneling microscopy (STM) studies at the interface between the basal plane of graphite and organic solutions or melts of long chain alkanes and alkyl derivatives reveal that the molecules order in lamellae with the main molecular axes oriented parallel to the substrate. Here we employ molecular dynamics (MD) simulations to obtain more details on the molecular order and dynamics within the alkane lamellae as a function of density. We find that the orientation of the molecular carbon zigzag planes relative to the graphite is governed by a subtle interplay of packing and entropic effects. In addition, we consider multiple layer adsorption and investigate the rapid loss of order with increasing distance from the interface. Finally, we study the diffusive behavior of an isolated long chain alkane, $C_{350}H_{702}$, on graphite, which is of interest in the context of STM imaging of isolated macromolecules at interfaces. The sensitive dependence on atomic parameters renders MD simulations a valuable complementary tool for the detailed interpretation of STM data.

I. INTRODUCTION

The molecular structure and dynamics at the interface between a flat solid surface and a complex fluid is of considerable interest, e.g., in the context of lubrication, adhesion, molecular recognition phenomena at interfaces, or for the organization of molecules possibly undergoing topochemical reactions. Recent scanning tunneling microscopy (STM) studies at the interface between organic solutions or melts of long chain alkanes and simple alkyl derivatives and the basal plane of graphite reveal highly ordered lamellar structures.[1-5] The STM images (two examples are shown in Fig. 1) confirm an earlier model proposed on the basis of adsorption isotherm and enthalpy measurements. It suggests that over a considerable range of concentrations the solute molecules physisorb in all-*trans* conformation parallel to the surface, forming densely packed monolayers.[6,7] A detailed analysis of the STM results allows, in addition, to determine the commensurability between substrate and adsorbate lattices, both along the molecular axes of the adsorbate as well as along the lamellae.[3] The time resolution of the STM experiment, however, is limited to the millisecond time scale. While this is sufficient to observe the cooperative reorganization of a few molecules within the monolayers,[2,3] it is far too slow to observe the intramolecular dynamics in this case. Here we combine STM results with computer simulations to obtain further insight.

Computer simulations are now among the standard theoretical approaches to adsorption phenomena on solid surfaces. Methods like Monte Carlo or molecular dynamics (MD) are useful tools in the study of the translational and orientational ordering of adsorbates, their commensurability or incommensurability with the substrate, the dynamics of adsorbates, and the universal and nonuniversal aspects of surface phase transitions (e.g., Refs. 8–11). Particularly, physisorption on graphite has been modeled for a number of adsorbate species like rare gas atoms (e.g., Kr[12] and Ar[13]), small linear molecules (e.g., N_2[14] and CS_2[15]), polar molecules (e.g., CH_3F and CH_3Cl[16]), and various hydrocarbons (methane,[17] ethylene,[18] ethane,[19] benzene,[20] butane, and decane[21]). The focus is hereby mainly on the calculation of structural phase diagrams in terms of temperature and coverage, on the energetics of adsorption, and on dynamical aspects like translational and rotational diffusion.

In the present work, an atomic model for the intra adsorbate and adsorbate–substrate interaction is combined with unit cell geometries and surface packing densities as obtained by STM, in order to yield insight into the entropics and energetics of long chain alkane layers. The main difference between previous simulations of alkanes physisorbed on graphite[21] and the present work is the high lateral packing density inside the molecular films considered here. The previous studies consider isotropic two-dimensional alkane fluids, whereas the present structures are almost closely packed. Although crystalline packings can often be predicted based on steric considerations alone, we find that subtle entropic effects in conjunction with small lateral density changes can strongly affect the structure of the adsorbate.

Using $C_{24}H_{50}$ as an example, we show that the interplay between entropy loss due to the molecular confinement and the energy of adsorption plays an important role for the orientational and positional order of the chains within the lamellae. This is useful in distinguishing different model structures which cannot be conclusively distinguished via STM alone. Furthermore, the simulated alkanes are not always aligned along a carbon chain direction in the graphite plane and neither are they always in registry with the graphite lattice, although this is energetically favorable. Instead, the chain dynamics together with the high packing density may cause communal tilting of the molecular axes inside a lamella. This effect is confirmed by corresponding STM ex-

 0021-9606/92/086213-09$06.00

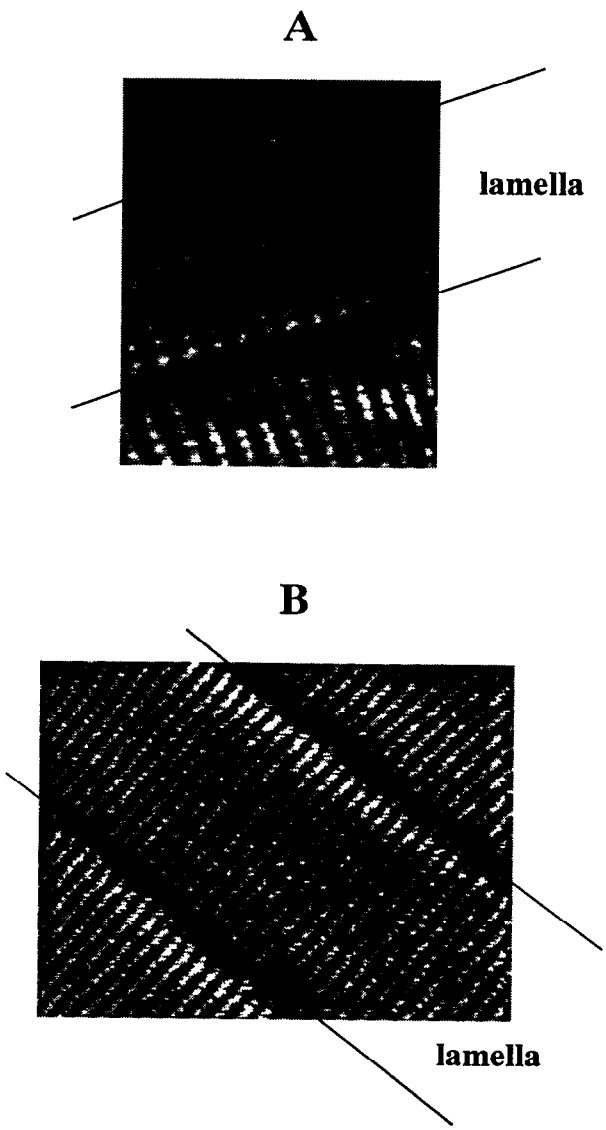

FIG. 1. STM images of $C_{24}H_{50}$ and $C_{50}H_{102}$ monolayers physisorbed at the interface between the basal plane of graphite and a 1-phenyloctane solution. The molecules are oriented perpendicular to the lamella boundaries indicated by the straight lines.

periments. In addition, STM, like many other techniques sensitive to the lateral surface structure, is less suited for probing the profile of an adsorbed film normal to the substrate surface. Surface force microscopy (SFM), for comparison, reveals the growth of multilayers on the surface at higher concentrations;[22] however, a detailed analysis of their behavior remains difficult. Here we simulate the structure and dynamics of ordered films as a function of distance from the surface. We use four layers of $C_{24}H_{50}$ as an example. Finally, we consider the dynamics of an isolated long alkane chain, $C_{350}H_{702}$, physisorbed on graphite. This study is motivated by the interest in imaging single macromolecules using STM.

II. METHOD

In the simplest case, MD stands for the numerical integration of the classical equations of motion governing the system of interest. Individual atoms (all atom method), as in our case, or clusters of atoms (united atom method) thereby interact via realistic potentials. The method provides a microscopic picture of the system in terms of spatial coordinates and time. For large enough systems and sufficiently long times, macroscopic observables, which can be compared to experimental measurements, can be derived from suitable averages based on the space-time trajectory of the system.

Our simulations were carried out based on the molecular mechanics and molecular dynamics subroutines provided with the AMBER molecular modeling package. For the type of problems studied here, however, it is advantageous to somewhat modify the AMBER force field to include an approximation that greatly reduces the computational effort. Within this approximation, the intra-adsorbate interactions are computed normally via the standard AMBER force field,[23] whereas the adsorbate–substrate interactions are treated in terms of a static adsorption potential corresponding to a perfectly ordered rigid substrate. This method assumes that the structural and dynamical properties of the adsorbate that are of interest are not significantly disturbed by the omission of the substrate dynamics, an assumption which has proven to yield good results in a number of related studies (cf. Ref. 21 and references therein). Thus, only the trajectory of the adsorbate is integrated, and the potential governing the motion of the adsorbate atoms takes the form

$$
\begin{aligned}
V = & \sum_{\text{bonds}} f_r (r - r_{\text{eq}})^2 + \sum_{\text{angles}} f_\delta (\delta - \delta_{\text{eq}})^2 \\
& + \sum_{\text{dihedral}} f_n \{1 + \cos(n\phi - \gamma)\} \\
& + \sum_{i<j} \sqrt{\epsilon_i \epsilon_j} \left\{ \left(\frac{\sigma_i + \sigma_j}{r_{ij}} \right)^{12} - 2 \left(\frac{\sigma_i + \sigma_j}{r_{ij}} \right)^{6} \right\} \\
& + \sum_{i<j} \frac{q_i q_j}{r_{ij}} + \sum_i V_{\text{surf}}(r_i).
\end{aligned}
\tag{1}
$$

The first three terms describe the bonding intra-adsorbate interactions (bond stretching, valence angle vibrations, and torsional vibrations). The remaining nonbonding intra-adsorbate terms are Lennard-Jones (LJ) interactions (using the Slater–Kirkwood rule to obtain the LJ parameters) and Coulomb interactions. The potential parameters entering into the intra adsorbate interactions are adopted from the AMBER data base, with the exception of the partial charges, which were calculated using the modified neglect of diatomic overlap (MNDO) method. The explicit parameter values used in the simulations are compiled in Table I.

The last term in Eq. (1) describes the external static potential due to the surface acting on the adsorbate atoms located at $\mathbf{r}_i = (x_i, y_i, z_i)$, where z_i is the normal distance from the surface. Steele[24] has shown that $V_{\text{surf}}(\mathbf{r}_i)$ can be expressed in terms of a simple, rapidly converging series. Assuming that the adsorbate substrate interactions are well

TABLE I. A summarization of the potential parameters entering into Eqs. (1)–(5).

Intra adsorbate parameters			
Bonds	f_r/kcal mol^{-1} Å^{-2}	r_{eq}/Å	
C–C	310	1.53	
C–H	331	1.09	
Angles	f_δ/kcal mol^{-1}	δ_{eq}	
C–C–C	40	109.5	
C–C–H	35	109.5	
H–C–H	35	109.5	
Dihedrals	f_n/kcal mol^{-1}	γ	n
x–C–C–x	1.3	0	3
LJ parameters	ϵ/kcal mol^{-1}	σ/Å	
C	0.12	1.85	
H	0.01	1.54	
Partial charges	$H_{0.004}$ $H_{0.004}$ $H_{0.005}$ $H_{-0.008}$		
	$\cdots C_{-0.008}-C_{-0.008}-C_{-0.027}-C_{0.041}-H_{-0.008}$		
LJ-parameters	ϵ/kcal mol^{-1}	σ/Å	
C–G	$6.28\,10^{-2}$	3.82	
H–G	$4.31\,10^{-2}$	3.37	
Substrate parameters			
$a_s = \sqrt{3}/2$	$a = 2.46$ Å	$d = 3.39$ Å	$g_1\ a = 4\pi/\sqrt{3}$

approximated by pairwise Lennard-Jones interactions, i.e., $\epsilon\{(\sigma/r)^{12} - 2(\sigma/r)^6\}$, and utilizing the translational symmetry of the substrate he obtains

$$V_{\text{surf}}(\mathbf{r}_i) = V_0(z_i) + \sum_{m=1}^{\infty} V_m(z_i) f_m(x_i, y_i)\,, \tag{2}$$

$$V_0(z_i) = \frac{2\pi\epsilon}{a_s a^2} \sum_{n=0}^{\infty} \left\{ \frac{\sigma^{12}}{5(z_i + nd)^{10}} - \frac{\sigma^6}{(z_i + nd)^4} \right\}, \tag{3}$$

$$V_m(z_i) = \frac{\pi\epsilon}{a_s a^2} \left\{ \frac{\sigma^{12} g_m^5}{1920 z_i^5} K_5(g_m z_i) - \frac{\sigma^6 g_m^2}{2 z_i^2} K_2(g_m z_i) \right\}, \tag{4}$$

where the expansion variable g_m is the magnitude of reciprocal lattice vectors corresponding to successively larger shells. Note that the LJ parameters ϵ and σ depend on the type of adsorbate atom at the position $\mathbf{r}_i$. Here $a_s a^2$ is the area of the graphite lattice unit cell, a is the magnitude of the graphite lattice vectors, d is the substrate layer separation, and K_ν is a Bessel function. The functions $f_m(x_i, y_i)$ characterize the symmetry of the substrate layers. For the basal plane of graphite, the $f_m(x_i, y_i)$ are tabulated up to $m = 5$.[24] However, including the two leading terms in Eq. (2) is sufficiently accurate (see also Ref. 25), and thus we only need

$$f_1(x_i, y_i) = -2\left\{ \cos\left(\frac{2\pi}{a}(x_i + y_i/\sqrt{3})\right) + \cos\left(\frac{2\pi}{a}(x_i - y_i/\sqrt{3})\right) + \cos\left(\frac{4\pi}{a} y_i/\sqrt{3}\right) \right\}. \tag{5}$$

Again, the numerical values of the parameters appearing in Eqs. (2)–(5) are listed in Table I. Note that the LJ parameters entering into the interaction of the hydrogens and the carbons with the graphite substrate are adopted from Battezati *et al.* (set B),[26] who obtain their parameters from fits to adsorption potentials derived by Kiselev *et al.*[27,28] Using Steel's potential, Battezati *et al.*[26] obtain good agreement for the isosteric heat of adsorption of various small hydrocarbon molecules on graphite.

In Fig. 2, the adsorption potential $\Sigma_i V_{\text{surf}}(\mathbf{r}_i)$ is shown

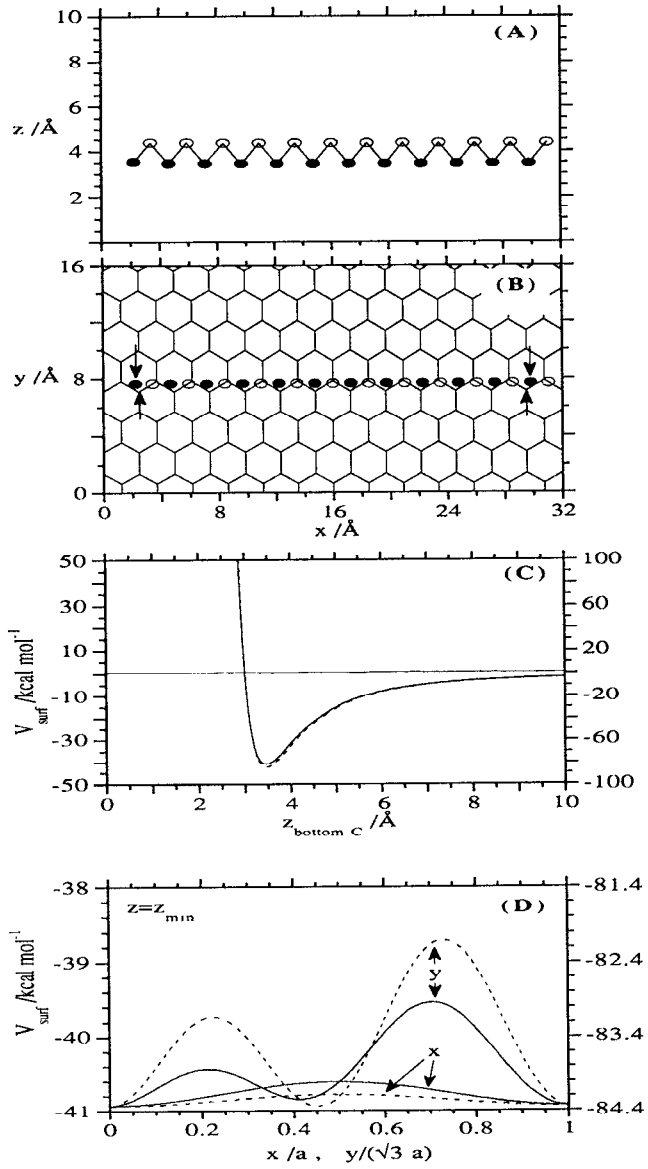

FIG. 2. The two upper panels show the optimized normal (A) and lateral (B) position of an isolated all-*trans* $C_{24}H_{50}$ molecule relative to the graphite surface, where circles indicate carbon atoms. The adsorption potential is calculated using Eqs. (2)–(5) with $m \leqslant 1$ while constraining the zigzag plane to be perpendicular to the surface. The arrows in panel (B) show the mismatch of the chain carbons with respect to the graphite lattice. The two bottom panels show the variation of the adsorption potential corresponding to normal (C) and lateral (D) translations. z_{bottomC} [cf. (C)] is the separation of the bottom chain carbons (solid circles) from the graphite surface and $z_{\min}$ [cf. (D)] refers to the potential minimum at $x = y = 0$. Note that the solid lines together with the left ordinate are for $C_{24}H_{50}$, whereas the dashed lines together with the right ordinate show the analogous results for $C_{50}H_{102}$.

for two different isolated alkane molecules, $C_{24}H_{50}$ [cf. panels (A)–(D)] and $C_{50}H_{102}$ [cf. panels (C) and (D)], adsorbed parallel to the surface in x direction with their carbon zigzag plane perpendicular to the surface. Notice the rather weak lateral modulation of the adsorbate–substrate interaction in comparison to the much stronger dependence on the adsorbate–substrate separation. It is also interesting to note that due to the small mismatch between the graphite lattice and the chain carbons [cf. Fig. 2(B)], the short chain has to overcome a larger potential barrier than the long chain when sliding along the x direction [cf. Fig. 2(D)].

Ideally, the simulation should include the adsorption from solution and the attendant formation of the lamellar structures. However, such a complete study is presently ruled out by the rather short time scales accessible with MD. Therefore, we must choose an initial structure which is already close to the equilibrium structure at the given conditions and to restrict ourselves to the study of accessible structural and dynamical effects. Each simulation is therefore based on an initial configuration whose unit cell symmetry and dimensions are deduced from STM images of the corresponding systems. Using equations (1)–(5), i.e., including all interactions, the potential energy of this initial structure is minimized employing a combination of the steepest descent and the conjugated gradient method. Here and in the succeeding MD runs we employ periodic boundary conditions parallel to the surface. The energy minimization has little effect on the structural arrangement in the plane of the surface. It mainly serves to optimize the adsorbate–substrate separation and, in the case of multilayer adsorption, the intra adsorbate layer spacing. The actual MD runs are then started from the so prepared optimized configurations. The atomic equations of motion of the adsorbate are solved using a leap-frog version of the Verlet–Störmer algorithm with a 10^{-3} ps time step. Throughout our simulations we employ the NVT ensemble (i.e., particle number, volume, and temperature are kept constant). Constant temperature is maintained according to the method of Berendsen *et al.*[29] using velocity rescaling with a temperature relaxation time of 0.1 ps. In addition, all nonbonded interactions are omitted beyond a residue based cut off at 8 Å, i.e., only the nonbonded interactions between residues which are wholly or partially contained within the cut-off sphere are included. Note in this context that for the present systems Coulomb interactions are small compared to the short ranged van der Waals interactions.

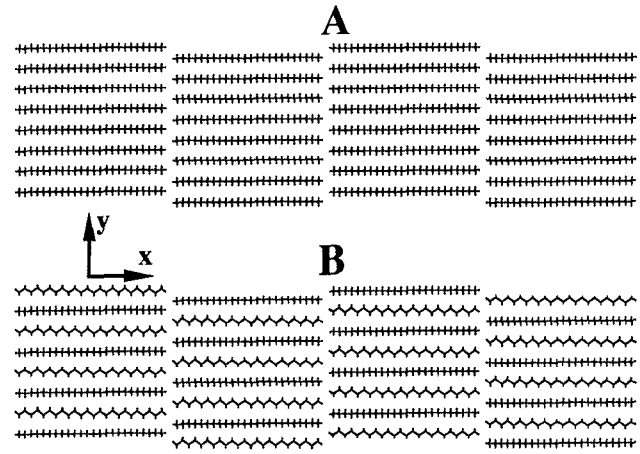

FIG. 3. Panel (A): Sketch of the initial structure consisting of 32 $C_{24}H_{50}$ molecules. The alkanes are in the all-*trans* conformation with their zigzag plane perpendicular to the graphite surface. The unit cell vectors are $(0, \sqrt{3}\,a)$ and $(13\,a, \sqrt{3}/2\,a)$, where $a = 2.46$ Å is the graphite lattice constant. The lateral position of the molecules corresponds to the optimized position shown in Fig. 2 (B). Panel (B): The same initial configuration as in panel (A), except that every second molecule is rotated by 90° with respect to its long axis.

III. RESULTS AND DISCUSSION

A. Monolayers

Earlier models of the structures formed by alkanes on graphite (based on adsorption isotherm[7] and STM measurements[1]) assumed that the carbon zigzag planes of all-*trans* alkanes are oriented parallel to the graphite basal plane. Contrary to this, more recent STM studies suggest that the zigzag planes are oriented perpendicular to the graphite surface.[3] Here we show that a theoretical approach to this and related questions based solely on potential energy considerations is insufficient because of the importance of entropic effects. We have modeled the dynamical evolution of two slightly different initial structures formed by $C_{24}H_{50}$ molecules. Sketches of the two initial structures are shown in Fig. 3. Both configurations are identical with respect to their geometry and the dimensions of their unit cell, which were chosen in accordance with the STM images. However, structure (A) consists of $C_{24}H_{50}$ molecules which are in their all-*trans* conformation with their zigzag planes oriented perpendicular to the graphite. Structure (B), on the other hand, differs from (A) in that the zigzag plane of every second molecule (in each lamella) is oriented parallel to the graphite. A configuration with all zigzag planes parallel to the graphite plane could not be simulated because the resulting exaggerated density in y direction leads to numerical instabilities. Using Eqs. (2)–(5), minimization of the potential energy of the two structures A and B yields the molecular adsorption energies -44.1 kcal/mol (A) and -46.1 kcal/mol (B). Thus, structure (B) is energetically favored. Note again that the minimization of the potential energy mainly affects the surface-adsorbate separation and does not significantly distort the initial structure parallel to the surface. However, even though structure (B) is energetically favored it is not necessarily thermally stable. This is illustrated in Fig. 4, which shows the result of two MD simulations for two different temperatures starting from the energetically optimized configuration (B). Figure 4 shows the number of molecules whose zigzag plane is oriented perpendicular to the surface divided by the total number of molecules. (The orientation of a molecule's zigzag plane is determined by inspection of ensemble snapshots on a graphite display.) For the higher temperature, $T = 400$ K, this ratio increases rapidly from 0.5 to 0.9 within ~ 30 ps. For the lower temperature, $T = 300$ K, the increase of the number of perpendicular chains is less pronounced within the simulated time interval.

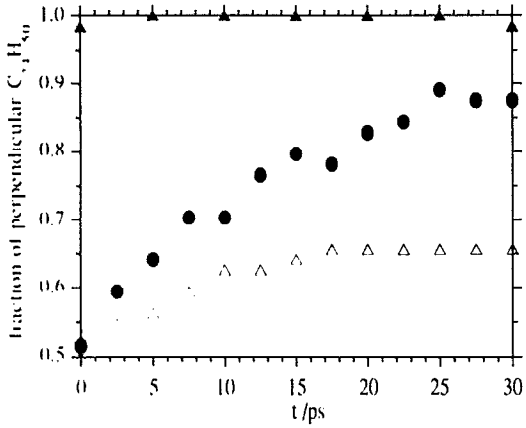

FIG. 4. Total fraction of $C_{24}H_{50}$ molecules whose molecular plane is perpendicular to the graphite surface vs simulation time. (solid triangles): the initial structure is (A) and $T = 300$ K; (open triangles): the initial structure is (B) and $T = 300$ K; (solid circles): the initial structure is (B) and $T = 400$ K. Note that simulation time range shown here is preceded by a 5 ps thermalization.

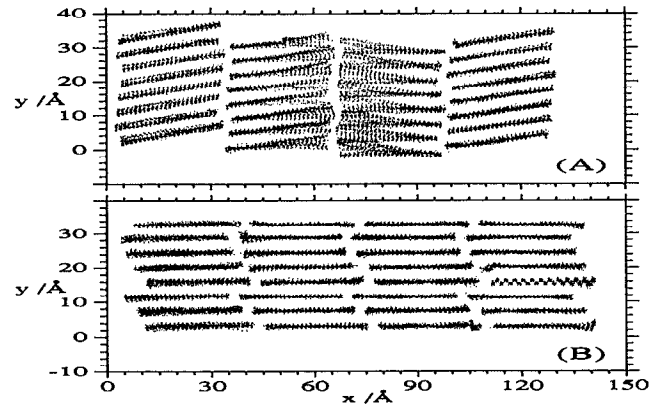

FIG. 6. Density plot showing the position of the chain carbons (indicated by dots) in the time interval between 60 ps and 80 ps. Panel (A) is based on the initial structure shown in Fig. 3 (A). Panel (B) is based on the same initial structure, which is, however, expanded by ~4% in x direction.

The orientation kinetics is considerably slower at this temperature. For the same temperature, $T = 300$ K, Fig. 4 also shows the result of a MD simulation starting from the optimized structure (A), where all molecular zigzag planes are initially perpendicular to the graphite surface. Note that throughout this simulation there is no significant deviations from the initial "all-up" configuration. The result of the above MD run at 400 K is illustrated independently in Fig. 5, which shows the distribution of the adsorbate carbon atoms as a function of distance from the surface. The two curves correspond to averages based on the initial 2 ps and final 6 ps of the time interval shown in Fig. 4. Notice that the final distribution exhibits nearly symmetrical double peaks indicating perpendicularly oriented zigzag planes. Unfortunately, a completely satisfactory explanation of the results in Figs. 4 and 5 requires detailed consideration of the subtle

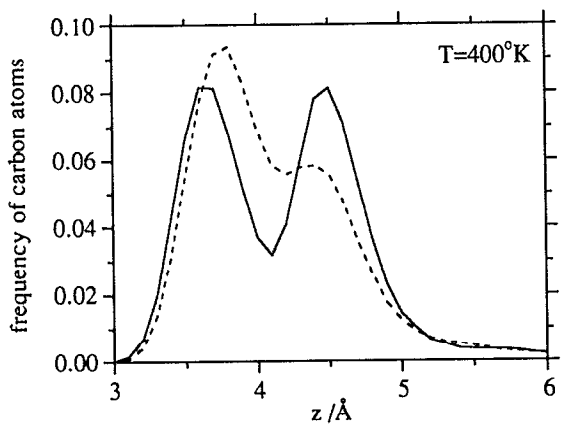

FIG. 5. Position distribution of the adsorbate carbon atoms as a function of the distance z from the graphite surface at $T = 400$ K. The solid line and the dashed line are the results of positional averages over the first 2 ps and the final 6 ps on the time axis of Fig. 4, respectively.

atomic interactions. However, it is safe to say that the entropy loss due to the greater lateral translational and conformational confinement imposed by structure B (due to the slightly higher packing density along the surface) is not compensated by the more negative average molecular adsorption energy.

Another example for the pronounced effects that small changes of the surface density may have on the lamellar structure is shown in Fig. 6. Figure 6 (A) shows a density plot of the adsorbate carbon atoms including the final 20 ps of a 80 ps simulation at $T = 300$ K starting from the initial structure sketched in Fig. 3 (A). Although the unit cell is commensurate with the substrate, the molecules do not strictly align along the energetically favorable x direction of the graphite lattice [cf. Fig. 2 (B)]. Instead, we obtain a slight communal tilt of the molecules within the same lamella with respect to the x direction. Corresponding tilts may indeed be observed experimentally. An example is shown in Fig. 7 (A). The experimentally observed tilts in fact exhibit dynamical behavior, i.e., it is possible to observe communal tilt flips between the "tilted" lamella and the "straight" lamella [cf. fig. 7 (B)]. Unfortunately, this type of dynamics is beyond the MD time scale. The occurrence of a tilt, however, is caused by the dense packing along the x direction. This can be demonstrated by a simulation differing from the above one only by a 4% extension of the unit cell along the x direction, i.e., the lamellar width is increased from $13a$ to $13.5a$. Both values are within the experimental range of spatial accuracy. The high density structure in Fig. 6 (A) differs strongly from the one obtained for the lower density shown in Fig. 6 (B). Notice that the intercalation of the chain ends in adjacent lamellae is abandoned and the chains are now strictly aligned along the x direction. In addition, the lamellar boundaries assume a fuzzy appearance. It is worth noting, however, that we do not find evidence for a liquid crystalline phase, i.e., fluid behavior along the long chain axis similar to a bulk columnar liquid crystalline mesophase. However, liquid crystalline behavior of large mole-

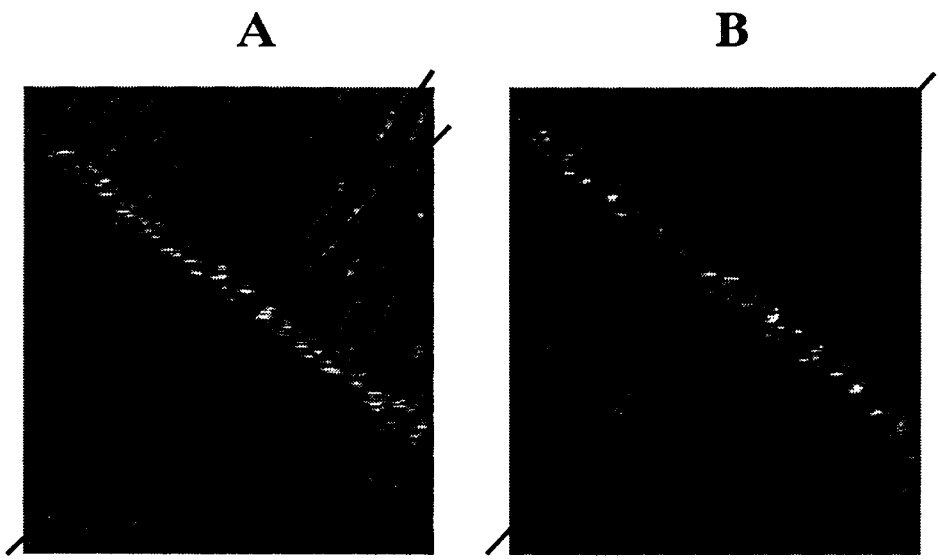

FIG. 7. Panel (A): STM image of $C_{50}H_{102}$ physisorbed on graphite [cf. Fig. 1 (B)]. This image shows two adjacent lamellae, where the molecules in the two lamellae are tilted with respect to each other. This is indicated by the two straight lines drawn parallel to the molecular backbones in the two lamellae. Panel (B): A subsequent scan of the same area shows aligned molecular backbones in both lamellae.

cules at high densities is slow compared to our time scale (e.g., Ref. 30), and thus such a transition can not be ruled out conclusively. Most importantly though, the small change in the unit cell size induces a structure which is inconsistent with the experimental results (e.g., cf. Figs. 1 and 7).

B. Multiple layers

Thus far, the STM results on ordered molecular films physisorbed on graphite were obtained on monolayers. Although multilayer adsorption is possible at higher solute concentrations, it is difficult to probe physisorbed multilayered structures using STM. For instance, increasing the separation of the tunneling tip to the substrate rapidly reduces the tunnel current, and thus the tip-to-surface separation is difficult to control. While studies employing surface force microscopy[22] or the surface force apparatus[31] may be better suited for that purpose, it remains a difficulty that the presence of the tip may cause local molecular disordering in the more weakly adsorbed layers above the first layer. Here the simulation can provide useful information on the behavior of the ordered films consisting of multiple layers as a function of separation from the substrate.

In the following, we model a $C_{24}H_{50}$ film adsorbed on graphite at $T = 300$ K including four ordered layers. Each layer of the equally spaced initial structure is identical to the initial structure for the monolayer shown in Fig. 3 (A) (except that here we only consider two lamellae consisting of four molecules each). The potential energy of this structure is minimized using Eqs. (1)–(5), which again mainly serves to adjust the interlayer and layer-surface separation (cf. above). The so optimized configuration is entered into the molecular dynamics simulation. During the MD runs, the motion of the molecules in the topmost adsorbate layer (as well as in lower layers) is constrained by a reflective hard planar wall located at height z_0. In reality, the halfspace above our topmost layer contains maybe further adsorbate layers, the adsorbate solution interface and, finally, the bulk solution. However, we chose this type of cut off because of the otherwise prohibitively large computational effort. In addition, a vacuum interface at the cut off is even less realistic due to the exaggerated chain dynamics in the absence of a constraining surface potential. Using the hard wall cut off, we can still obtain useful information on the adsorbate dynamics, if the layer closest to the wall serves as a buffer (cf. below) and is excluded from the analysis. This is reasonable, because the important atomic interactions are short ranged LJ interactions (cf. below). A good estimate for z_0 can be obtained based on the positions of the layers obtained via the minimization of the total potential energy.

Figure 8 (A) shows a density plot of the adsorbate carbon atoms as a function of their normal separation from the graphite surface for $C_{24}H_{50}$. Only three layers are shown—

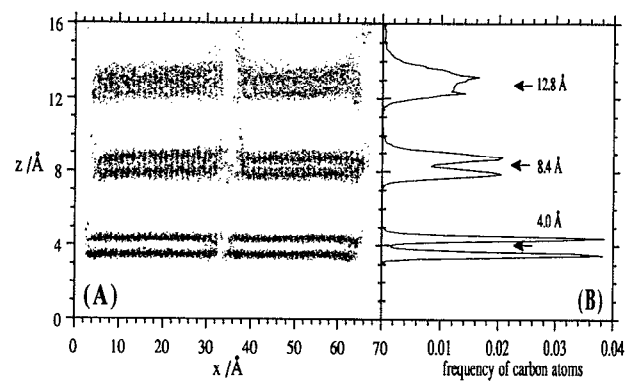

FIG. 8. Panel (A): Density plot of the chain carbons for $C_{24}H_{50}$ showing the distance from the surface vs the lateral coordinate x. The plot represents the superposition of 20 configurations in the time range between 70 and 90 ps. Panel (B): The frequency plot corresponding to panel (A). Notice, only three of a total of four layers are considered in the two panels. The position of the reflecting wall is $z_0 = 21.5$ Å.

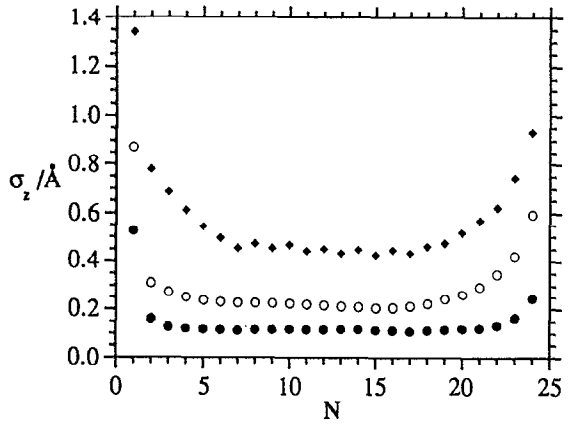

FIG. 9. Standard deviation σ_z of the normal position z of the alkane carbons above the surface corresponding to the three layers shown in Fig. 8. (solid circles): bottom layer; (open circles): second layer; (solid diamonds): third layer. N indicates the position of the carbon atoms within the molecule.

the topmost (fourth) layer is omitted as explained above. Notice that only the bottom layer is well localized normal to the surface, whereas already the second and the third layer are "smeared out." As shown in Fig. 8 (B), a major change in the perpendicular ordering occurs going from the first to the second layer, whereas the difference between the second and third layer is somewhat less pronounced. This is consistent with the narrow potential well shown in Fig. 2 (C). Here the reflecting wall is at $z_0 = 21.5$ Å. Varying this value by $\pm$ 1 Å does change the ordering within the layer closest to the wall, whereas the lower layers remain virtually unaffected. For the molecular adsorption energy within the bottom layer we find -37.3 ± 0.4 kcal/mol, which is, as expected, smaller than the corresponding value of -41 kcal/mol obtained in the idealized $T = 0$-case illustrated in Fig. 2. Because of the short range of the surface potential, the molecular adsorption energy due to the interaction with the substrate alone is only -3 kcal/mol within the second layer and decreases to -1 kcal/mol in the third layer. These values are calculated based on the increase of the total adsorption energy as a function of the number of layers obtained from additional simulation runs on a double layer and a triple layer configuration completely analogous to the quadruple layer case. Note also that the above values are consistent with what one would deduce from the potential shown in Fig. 2 (C) in conjunction with the layer positions shown in Fig. 8 (B). For a multilayered adsorbate, the adsorption energy of a molecule in a higher layer is, in addition, increased by the presence of the lower layers. Here, this increase of the molecular adsorption energy, which is mainly due to the van der Waals attractions between molecules in adjacent layers, is -2 kcal/mol per molecule and per layer in addition to the first layer. Analogous to the above case, this number follows directly from the increase of the (attractive) van der Waals contribution to the total potential energy as a function of the number of layers. In addition, we found that the lateral molecular interaction energy between molecules within the same layer, which is also almost exclusively due to van der Waals attractions, is about -6 kcal/mol. In this context it is also interesting to note that the molecules are well localized lateral to the graphite lattice (even in the second layer) as can be seen from the contrast modulation in the density plot along the x direction [cf. Fig. 8 (A)].

Finally, Fig. 9 shows the standard deviation σ_z of the z position of the alkane carbons corresponding to the three layers shown in Fig. 8. Notice that σ_z increases with increasing distance from the surface, as one might expect. However, notice also the significantly larger values of σ_z near the chain ends, and the increasing range of this end effect along the chain with increasing distance from the surface. This suggests that the fuzzy "channels" separating adjacent lamellae in the STM images (cf. Figs. 1 and 7) are due to the pronounced perpendicular mobility of the atoms near the chain ends. Similarly, one might speculate that this effect strongly diminishes the STM resolution, not only near the chain ends, but across the entire width of the lamella, if one attempts to image the more loosely bound second and third layer. It is worth noting that corresponding multilayer simulations for $C_{50}H_{102}$ give results very similar to those for $C_{24}H_{50}$. In particular, σ_z does not significantly depend on molecular weight under these conditions.

C. A single long alkane chain at the graphite-vacuum interface

Recently, considerable effort has been devoted to the imaging of physisorbed isolated macromolecules using STM. In this context it is interesting to model the behavior of a single large alkane chain physisorbed on graphite under vacuum. Here we consider $C_{350}H_{702}$ at $T = 300$ K using free boundary conditions. The initial conformation is the fully stretched chain with its zigzag plane parallel to the surface. Unlike in the case of the densely packed layers, the predominantly parallel orientation of the zigzag plane is now thermally stable. This is illustrated via the adsorbate carbon distribution as a function of separation from the surface shown in Fig. 10, which exhibits a single peak at $\sim$3.8 Å. Even though the occasional occurrence of perpendicularly oriented zigzag segments along the chain gives rise to a shoulder at $\sim$4.5 Å, there are no "loops" or "tails" extending into the vacuum during the entire 1 ns simulation. For the adsorption energy we find -533 ± 8 kcal/mol. However, interesting from the point of view of the STM experiment is the mobility of the chain along the surface. Figure 11 shows the root-mean-square displacement of the central carbon atoms, i.e., carbon atoms 1–50 and 300–350 are omitted to exclude end effects, parallel and perpendicular to the surface. In addition, the insert in Fig. 11 shows two chain conformations after 400 ps and 1000 ps of simulation time. As can be seen from the lateral rms displacement, imaging of a single alkane chain requires additional pinning of the chain, as provided inside a dense layer, or sufficiently low temperatures. Note that the carbon atoms in the single chain (under vacuum) are also much less localized perpendicular to the surface compared to the carbon atoms in the molecules forming the bottom layer of a multilayer arrangement (cf. Figs. 9 and 11).

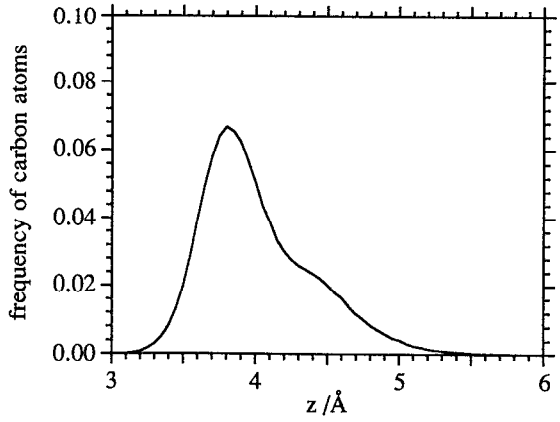

FIG. 10. Distribution of the carbon atoms of a single $C_{350}H_{702}$ molecule as a function of the distance z from the surface obtained by averaging over a 600 ps time interval after 400 ps of simulation.

IV. CONCLUSION

It has been demonstrated that MD simulations are a valuable complementary tool for the interpretation of STM data. Using the physisorption of alkanes on graphite as an example, the present work shows that a combination of STM and MD can be employed to describe in great detail the molecular structure and dynamics in ultrathin organic films. The level of understanding goes well beyond what any of the methods would acheive independently, since the accessible time scales are mutually exclusive. In particular, the orientation of the molecular planes with respect to the surface and the occurrence of communal tilting of the molecular axes with respect to the carbon chain direction in the graphite lattice has been analyzed. In addition, MD provides information on the average spatial localization of the alkane atoms as well as its variance as a function of the position along the chain and as a function of the distance from the substrate.

The focus of the present work is on a single type of adsorbate–substrate system. In future simulations we plan to extend our work to different substrates (e.g., mica,[31] MoS_2, etc.) and different adsorbates (cf. Refs. 2, 3, and 32) in order to determine the role of the surface geometry and the chemical composition on the resulting interfacial structures.

Finally, we want to point out that the major shortcoming of this type of simulation is the necessity of considerable experimental input regarding the equilibrium structure of the system of interest. While for small molecules MD allows the prediction of the equilibrium structure under certain given conditions (e.g., surface density, temperature, etc.), this is presently prohibited for a dense macromolecular structure, due to the excessive simulation time required for equilibration. In particular, the complex surface structures formed by more complicated molecules like, e.g., cyanobiphenyls,[33] phenylbenzoates, or triphenylenes[32] make the development of a theoretical approach, which allows to predict these structures, highly desirable.

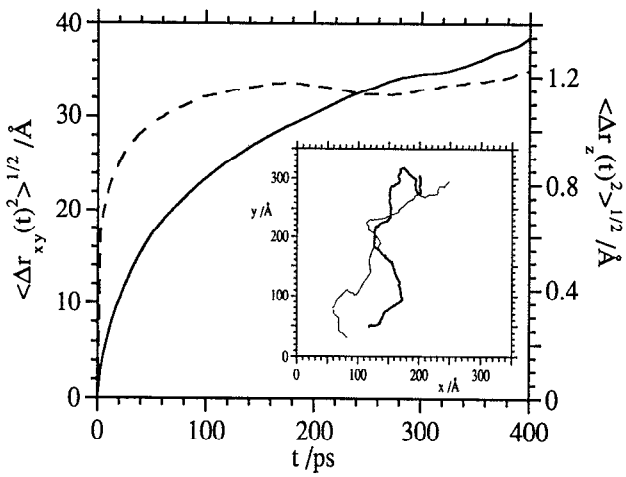

FIG. 11. RMS-displacement parallel (xy: solid line) and perpendicular (z: dashed line) to the graphite surface averaged over the central carbon atoms (i.e., the C atoms 1–50 and 300–350 are omitted) of a single $C_{350}H_{702}$ molecule at $T = 300$ K. The insert shows two conformations of after 400 ps (light) and 1000 ps (heavy) of simulation time.

ACKNOWLEDGMENT

The authors wish to thank S. Buchholz for recording the STM images.

[1] G. C. McGonigal, R. Bernhardt, D. J. Thomson, Appl. Phys. Lett. **57**, 28 (1990).
[2] J. P. Rabe and S. Buchholz, Phys. Rev. Lett. **66**, 2096 (1991).
[3] J. P. Rabe and S. Buchholz, Science **253**, 424 (1991).
[4] J. P. Rabe and S. Buchholz, Makromol. Chem. Macromol. Symp. **50**, 261 (1991).
[5] S. Buchholz and J. P. Rabe, Angew. Chem. **104**, 188 (1992).
[6] A. J. Groszek, Nature **196**, 531 (1962); *ibid.* **204**, 680 (1964); Proc. R. Soc. London, Ser. A **314**, 473 (1970).
[7] G. H. Findenegg and M. Liphard, Carbon **25**, 119 (1987).
[8] A. Zangwill, *Physics at Surfaces* (Cambridge University, Cambridge, 1988).
[9] F. F. Abraham, Rep. Prog. Phys. **45**, 1113 (1982).
[10] D. Nicholson and N. G. Parsonage, *Computer Simulations and the Statistical Mechanics of Adsorption* (Academic, New York, 1982).
[11] M. P. Allen and D. J. Tildesley, *Computer Simulations of Liquids* (Claredon, Oxford, 1990).
[12] F. F. Abraham, W. E. Rudge, D. J. Auerbach, and S. W. Kock, Phys. Rev. Lett. **52**, 445 (1984).
[13] L. A. Rowley, D. Nicholson, and N. G. Parsonage, Mol. Phys. **31**, 365 (1976).
[14] J. Talbot, D. J. Tildesley, and W. A. Steele, Mol. Phys. **51**, 1331 (1984).
[15] Y. P. Joshi, D. J. Tildesley, J. S. Ayres, and R. K. Thomas, Mol. Phys. **65**, 991 (1988).
[16] C. J. Ruiz-Suarez, M. L. Klein, M. A. Moller, P. A. Rowtree, G. Scoles, and J. Xu, Phys. Rev. Lett. **61**, 710 (1988).
[17] E. S. Severin and D. J. Tildesley, Mol. Phys. **41**, 1401 (1980).
[18] S. Nosé and M. L. Klein, Phys. Rev. Lett. **53**, 818 (1984).
[19] M. A. Moller and M. L. Klein, J. Chem. Phys. **90**, 1960 (1989).
[20] R. Hentschke and B. L. Schürmann, Surf. Sci. (in press).
[21] S. Leggetter and D. J. Tildesley, Mol. Phys. **68**, 519 (1989); Ber. Bunsenges. Phys. Chem. **94**, 285 (1990).
[22] L. M. Eng, H. Fuchs, S. Buchholz, J. P. Rabe, Ultramicroscopy (in press).
[23] S. J. Weiner, P. A. Kollman, D. A. Case, U. C. Singh, C. Ghio, G. Alagona, S. Profeta, and P. Weiner, J. Am. Chem. Soc. **106**, 765 (1984).
[24] W. A. Steele, Surf. Sci. **36**, 317 (1973).
[25] W. A. Steele, A. V. Vernov, and D. J. Tildesley, Carbon **25**, 7 (1987).
[26] L. Battezatti, C. Pisani, and F. Ricca, J. Chem. Soc. Faraday. Trans. II **71**, 1629 (1975).
[27] A. V. Kiselev and D. P. Poshkus, Trans. Faraday. Soc. **59**, 428 (1963).

[28] A. V. Kiselev, D. P. Poshkus, and A. Ya. Afreimovich, Russ. J. Phys. Chem. **42**, 1345 (1968).
[29] H. J. C. Berendsen, J. P. M. Postma, W. F. van Gunsteren, A. DiNola, and J. R. Haak, J. Chem. Phys. **81**, 3684 (1984).
[30] M. R. Wilson and M. P. Allen, Mol. Cryst. Liq. Cryst. **198**, 465 (1991).
[31] S. Granick, Science **253**, 1374 (1991).
[32] J. P. Rabe, in *Nanostructures Based on Molecular Materials*, edited by W. Göpel and Ch. Ziegler, (VCH, Weinheim, 1992, in press).
[33] D. P. E. Smith, J. K. H. Hörber, G. Binnig, and H. Nejoh, Nature **344**, 641 (1990).